

SUPPLEMENTARY MATERIAL

In Situ Spectroelectrochemical Investigations of Ru^{II} Complexes with Bispyrazolyl Methane Triarylamine Ligands

Carol Hua,^A Brendan F. Abrahams,^B Floriana Tuna,^C David Collison,^C and Deanna M. D'Alessandro^{A,D}

^ASchool of Chemistry, The University of Sydney, Sydney, NSW 2006, Australia.

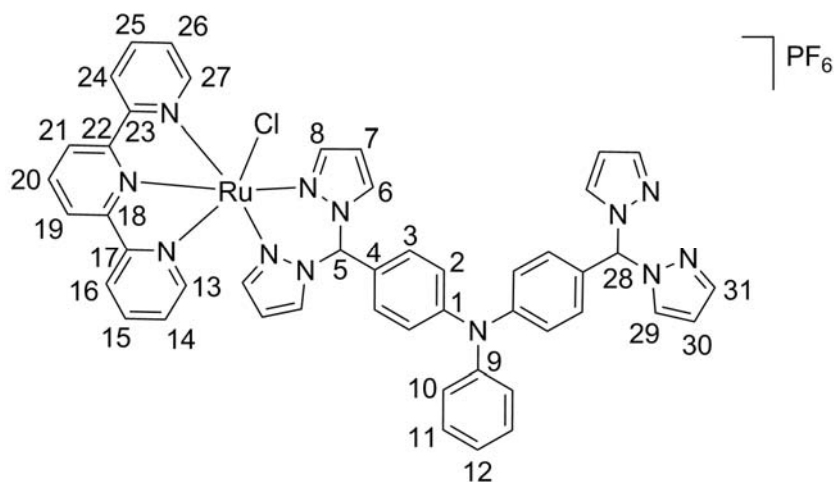
^BSchool of Chemistry, The University of Melbourne, Melbourne, Vic. 3010, Australia.

^CSchool of Chemistry, The University of Manchester, Manchester, M13 9PL, UK.

^DCorresponding author. Email: deanna.dalessandro@sydney.edu.au

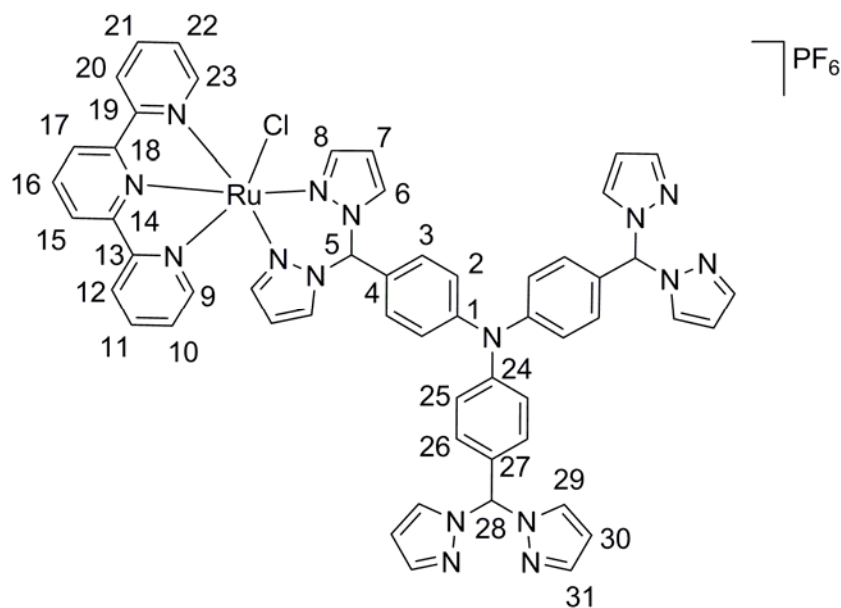
Experimental

[RuCl(tpy)(TPA-2bpm)]PF₆



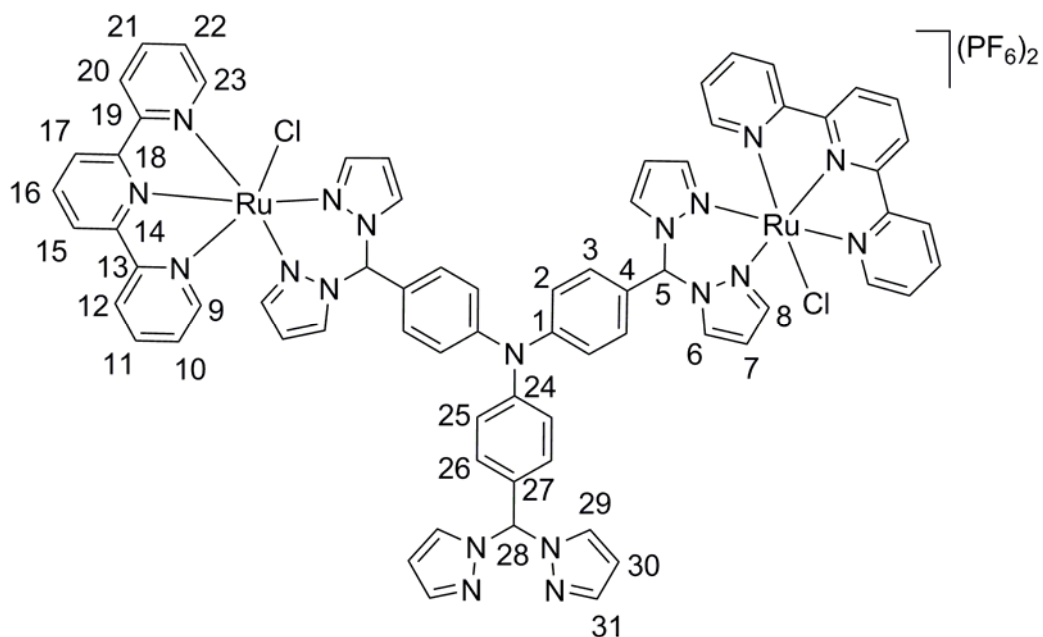
¹H NMR (CD₃CN, 500 MHz): δ 9.01 (d, ³J_{H-H} = 2.0 Hz, 2H, **H6/H8**), 8.43 (d, ³J_{H-H} = 2.0 Hz, 2H, **H6/H8**), 8.38 (d, ³J_{H-H} = 3.5 Hz, 1H, **H19**), 8.36 (d, ³J_{H-H} = 3.5 Hz, 1H, **H21**), 8.30 (d, ³J_{H-H} = 8.0 Hz, 1H, **H16**), 8.24 (d, ³J_{H-H} = 8.0 Hz, 1H, **H24**), 7.99 (t, ³J_{H-H} = 8.0 Hz, 1H, **H20**), 7.93 (s, 1H, **H5**), 7.83 (t, ³J_{H-H} = 8.0 Hz, 1H, **H15**), 7.79 (t, ³J_{H-H} = 8.0 Hz, 1H, **H25**), 7.76 (br s, 3H, **H21**, **H29/H31**), 7.62 (d, ³J_{H-H} = 8.0 Hz, 1H, **H13**), 7.55 (d, ³J_{H-H} = 8.0 Hz, 1H, **H27**), 7.38 (t, ³J_{H-H} = 8.0 Hz, 1H, **H14**), 7.33 (t, ³J_{H-H} = 6.0 Hz, 1H, **H12**), 7.18 (t, ³J_{H-H} = 6.0 Hz, 1H, **H26**), 7.11 (d, ³J_{H-H} = 8.5 Hz, 2H, **H10/H11**), 7.04 (d, ³J_{H-H} = 8.5 Hz, 2H, **H10/H11**), 6.96 (t, ³J_{H-H} = 2.5 Hz, 2H, **H7**), 6.77 (d, ³J_{H-H} = 8.5 Hz, 2H, **H2/H3**), 6.44 (d, ³J_{H-H} = 2.0 Hz, 2H, **H22/H24**), 6.26 (d, ³J_{H-H} = 8.0 Hz, 2H, **H2/H3**), 6.07 (t, ³J_{H-H} = 2.0 Hz, 2H, **H23**) ppm. ¹³C{¹H} NMR (CD₃CN, 125 MHz): δ 161.2 (**C18**), 161.1 (**C22**), 160.0 (**C17**), 159.6 (**C23**), 154.5 (**C9**), 149.9 (**C22/C24**), 148.7 (**C1**), 148.2 (**C6/C8**), 145.9 (**C6/C8**), 141.3 (**C13**), 137.7 (**C6/C8**, **C15**, **C29/C31**, **C28**), 137.0 (**C15'**), 134.6 (**C20**), 130.9 (**C14**), 130.8 (**C13'**), 129.4 (**C10/C11**), 128.1 (**C12**), 127.9 (**C4**), 127.5 (**C10/C11**), 126.3 (**C14'**), 124.4 (**C16**), 124.1 (**C16'**), 123.1 (**C19**), 123.0 (**C19'**), 121.6 (**C2/C3**), 109.0 (**C7**), 108.8 (**C30**), 107.2 (**C2/C3**), 77.7 (**C21**), 76.5 (**C5**) ppm. Elemental Analysis: Found C, 53.54; H, 3.52 and N, 15.82%; Calculated for C₄₇H₃₈ClF₆N₁₂PRu: C, 53.64; H, 3.64; N, 15.97%. ESI-MS (ESI⁺, MeOH): 906.93 (Calculated [M-PF₆]⁺ = 907.21, 100%) amu.

[RuCl(tpy)(TPA-3bpm)]PF₆



¹H NMR (CD₃CN, 500 MHz): δ 9.01 (br s, 2H, **H6/H8**), 8.46 (br s, 2H, **H6/H8**), 8.39 (t, ³J_{H-H} = 3.8 Hz, 1H, **H16**), 8.32 (d, ³J_{H-H} = 8.5 Hz, 1H, **H12**), 8.25 (d, ³J_{H-H} = 8.5 Hz, 1H, **H20**), 8.03-7.95 (m, 2H, **H15**, **H17**), 7.95 (s, 1H, **H5**), 7.87 (t, ³J_{H-H} = 8.5 Hz, 1H, **H11**), 7.79 (br s, 4H, **H29/H31**), 7.77 (s, 2H, **H28**), 7.75 (t, ³J_{H-H} = 8.5 Hz, 1H, **H21**), 7.64 (d, ³J_{H-H} = 8.5 Hz, 1H, **H9**), 7.56 (t, ³J_{H-H} = 8.5 Hz, 1H, **H22**), 7.34 (t, ³J_{H-H} = 8.5 Hz, 1H, **H10**), 7.11 (d, ³J_{H-H} = 8.5 Hz, 4H, **H25/H26**), 7.09 (d, ³J_{H-H} = 8.5 Hz, 1H, **H23**), 7.07 (d, ³J_{H-H} = 8.5 Hz, 4H, **H25/H26**), 6.96 (t, ³J_{H-H} = 2.0 Hz, 2H, **H7**), 6.83 (d, ³J_{H-H} = 8.5 Hz, 2H, **H3**), 6.45 (d, ³J_{H-H} = 2.0 Hz, 4H, **H29/H31**), 6.30 (d, ³J_{H-H} = 8.5 Hz, 2H, **H2**), 6.08 (t, ³J_{H-H} = 2.0 Hz, 2H, **H30**) ppm. ¹³C{¹H} NMR (CD₃CN, 125 MHz): δ 161.3 (**C14/C18**), 161.2 (**C14/C18**), 160.1 (**C13/C19**), 159.8 (**C13/C19**), 154.7 (**C24**), 153.5 (**C1**), 148.8 (**C6/C8**), 146.0 (**C29/C30**), 141.4 (**C22**), 137.8 (**C6/C8**), 137.7 (**C29/C31**), 137.7 (**C11**), 137.1 (**C21**), 134.7 (**C15**, **C17**), 133.6 (**C2**), 131.0 (**C9**), 129.7 (**C25**), 130.1 (**C27**), 128.2 (**C4**), 128.1 (**C10**), 127.5 (**C23**), 126.3 (**C26**), 125.0 (**C12**), 124.5 (**C20**), 123.1 (**C16**), 122.6 (**C3**), 109.1 (**C7**), 108.7 (**C30**), 107.3 (**C2/C3**), 77.8 (**C28**), 76.6 (**C5**) ppm. Elemental Analysis: Found C, 54.25; H, 3.95 and N, 18.72; Calculated for C₅₄H₄₄ClF₆N₁₆PRu: C, 54.12; H, 3.70; N, 18.70%. ESI-MS (ESI⁺, MeOH): 1053.13 (Calculated [M-PF₆]⁺ = 1053.27, 100%) amu.

[Ru₂Cl₂(tpy)₂(TPA-3bpm)](PF₆)₂



¹H NMR (CD₃CN, 500 MHz): δ 9.02 (d, ³J_{H-H} = 2.0 Hz, 1H, **H6/H8**), 8.57 (d, ³J_{H-H} = 2.0 Hz, 4H, **H6/H8**), 8.42-8.38 (m, 4H, **H15** and **H17**), 8.33 (d, ³J_{H-H} = 8.0 Hz, 2H, **H12**), 8.23 (d, ³J_{H-H} = 8.0 Hz, 2H, **H20**), 8.17 (s, 1H, **H28**), 8.01 (t, ³J_{H-H} = 8.0 Hz, 2H, **H16**), 7.90-7.87 (m, 6H, **H29/H31**, **H11**), 7.83 (s, 2H, H5), 7.66-7.64 (m, 2H, **H21**), 7.56-7.54 (m, 2H, **H9**), 7.49 (d, ³J_{H-H} = 5.5 Hz, 2H, **H23**), 7.34 (t, ³J_{H-H} = 7.0 Hz, 2H, **H10**), 7.19-7.16 (m, 4H, **H25**, **H26**), 6.99 (t, ³J_{H-H} = 2.0 Hz, 2H, **H7**), 6.95 (t, ³J_{H-H} = 7.0 Hz, 2H, **H22**), 6.82 (d, ³J_{H-H} = 8.5 Hz, 4H, **H2/H3**), 6.47 (d, ³J_{H-H} = 2.0 Hz, 2H, **H29/H31**), 6.253 (d, ³J_{H-H} = 8.5 Hz, 4H, **H2/H3**), 6.12 (t, ³J_{H-H} = 2.0 Hz, 2H, **H30**) ppm. ¹³C{¹H} NMR (CD₃CN, 125 MHz): δ 161.4 (**C14/C18**), 161.3 (**C14/C18**), 160.0 (**C13**), 159.8 (**C19**), 148.9 (**C4**), 148.8 (**C6/C8**), 147.2 (**C27**), 146.2 (**C29/C31**), 141.5 (**C9**), 141.4 (**C23**), 138.1 (**C11**), 138.1 (**C6/C8**), 137.9 (**C29/C31**), 134.8 (**C16**), 131.1 (**C21**), 131.0 (**C1**), 130.1 (**C24**), 129.7 (**C25/C26**), 128.3 (**C10**), 128.3 (**C25/C26**), 127.8 (**C2/C3**), 126.3 (**C22**), 124.6 (**C12**), 123.9 (**C20**), 123.8 (**C2/C3**), 123.2 (**C15/C17**), 123.1 (**C15/C17**), 109.2 (**C30**), 108.9 (**C7**), 77.7 (**C5**), 76.4 (**C28**) ppm. Elemental Analysis: Found C, 48.21; H, 3.22 and N, 15.73; Calculated for C₆₉H₅₅Cl₂F₁₂N₁₉P₂Ru₂: C, 48.37; H, 3.24; N, 15.53%. ESI-MS (ESI⁺, MeOH): 712.33 (Calculated [M-2PF₆]²⁺ = 711.62, 100%) amu.

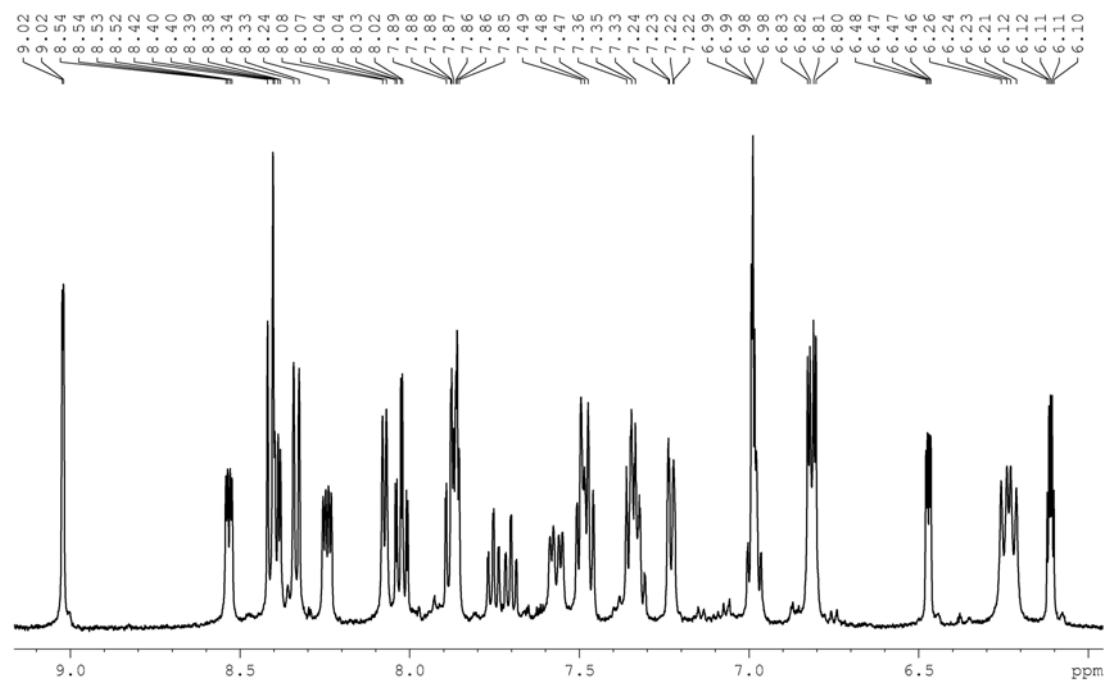


Figure S1. Solution state ^1H NMR spectrum of $[\text{Ru}_2\text{Cl}_2(\text{tpy})_2(\text{TPA-2bpm})](\text{PF}_6)_2$ recorded at 500 MHz in CD_3CN .

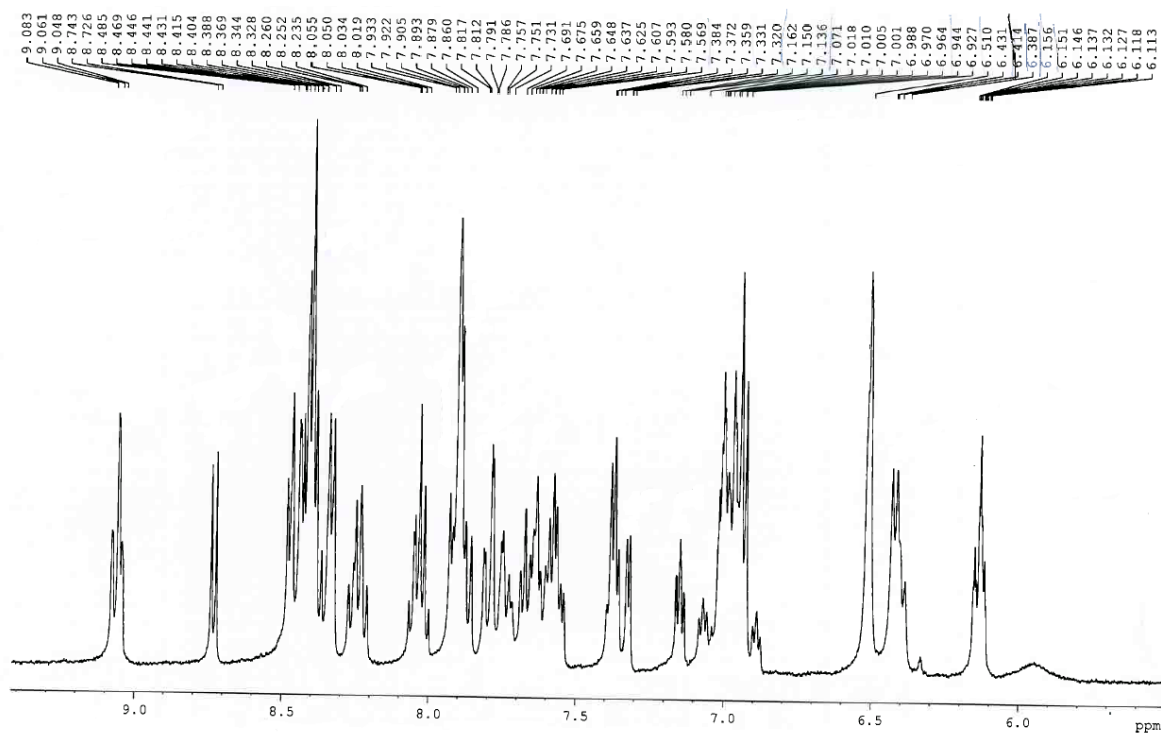


Figure S2. Solution state ^1H NMR spectrum of $[\text{Ru}_3\text{Cl}_3(\text{tpy})_3(\text{TPA-3bpm})](\text{PF}_6)_3$ recorded at 500 MHz in CD_3CN .

Table A1.1. Crystal data and structure refinement details for **TPA-2bpm**

Parameter	
Formula	C ₃₂ H ₂₇ N ₉
M/g mol ⁻¹	537.63
Temperature (K)	150(2)
Crystal system	Triclinic
Crystal size (mm ³)	0.188 × 0.144 × 0.100
Crystal colour	Colourless
Crystal Habit	Block
<i>a</i> (Å)	9.9607(3)
<i>b</i> (Å)	12.2145(3)
<i>c</i> (Å)	12.9010(4)
<i>α</i> (°)	110.727(3)
<i>β</i> (°)	102.826(2)
<i>γ</i> (°)	101.316(2)
<i>V</i> (Å ³)	1364.85(7)
<i>Z</i>	2
ρ_{calc} (mg/mm ³)	1.308
λ (CuK α)	1.54178 Å
μ (CuK α)	0.652 mm ⁻¹
$T(\text{CRYALISPRO})_{\text{min,max}}$	0.93508, 1.000000
$2\theta_{\text{max}}$	151.82°
hkl range	-12 12, -15 14, -16 16
Reflections collected	24161/5651[R(int) = 0.0196]
Data/parameters	5022/370
Final R indexes [all data]	R ₁ = 0.0557, wR ₂ = 0.1369
Goodness-of-fit on F ²	1.076
Residual Extrema	-0.508, 0.570 e ⁻ Å ⁻³

* $R1 = \frac{\sum ||F_o| - |F_c||}{\sum |F_o|}$ for $F_o > 2\sigma(F_o)$; $wR2 = \frac{(\sum w(F_o^2 - F_c^2)^2)}{\sum (wF_c^2)^2}^{1/2}$
all reflections
 $w = 1/[\sigma^2(F_o^2) + (0.0452P)^2 + 0.9594P]$ where $P = (F_o^2 + 2F_c^2)/3$

Table A1.2. Crystal data and structure refinement details for **TPA-3bpm**

Parameter	
Formula	C ₃₉ H ₃₃ N ₁₃ O _{1.62}
M/g mol ⁻¹	709.65
Temperature (K)	100(1)
Crystal system	Hexagonal
Crystal size (mm ³)	0.10 × 0.10 × 0.06
Crystal colour	Colourless
Crystal Habit	plate
<i>a</i> (Å)	11.903(2)
<i>b</i> (Å)	11.903(2)
<i>c</i> (Å)	14.466(3)
γ (°)	120
V (Å ³)	1775.0(7)
Z	2
ρ _{calc} (mg/mm ³)	1.328
λ(Synchrotron)	0.7109 Å
μ(Synchrotron)	0.087 mm ⁻¹
hkl range	-15 15, -15 15, -18 18
Reflections collected	27876/1410[R(int) = 0.0701]
Data/parameters	1286/152
Final R indexes [all data]	R ₁ = 0.0761, wR ₂ = 0.1801
Goodness-of-fit on F ²	1.124
Residual Extrema	-0.186, 0.189 e ⁻ Å ⁻³

$$RI = \Sigma(|F_o| - |F_c|)/\Sigma(|F_o|); wR_2 = [\Sigma\{w(F_o^2 - F_c^2)^2/\Sigma\{w(F_o^2)^2\}}]^{1/2}, wR2 = (\Sigma w(F_o^2 - F_c^2)^2/S(wF_c^2)^2)^{1/2} \quad \text{all reflections} \quad w=1/[s^2(F_o^2)+(0.0560P)^2+1.1154P] \quad \text{where} \\ P=(F_o^2+2F_c^2)/3$$

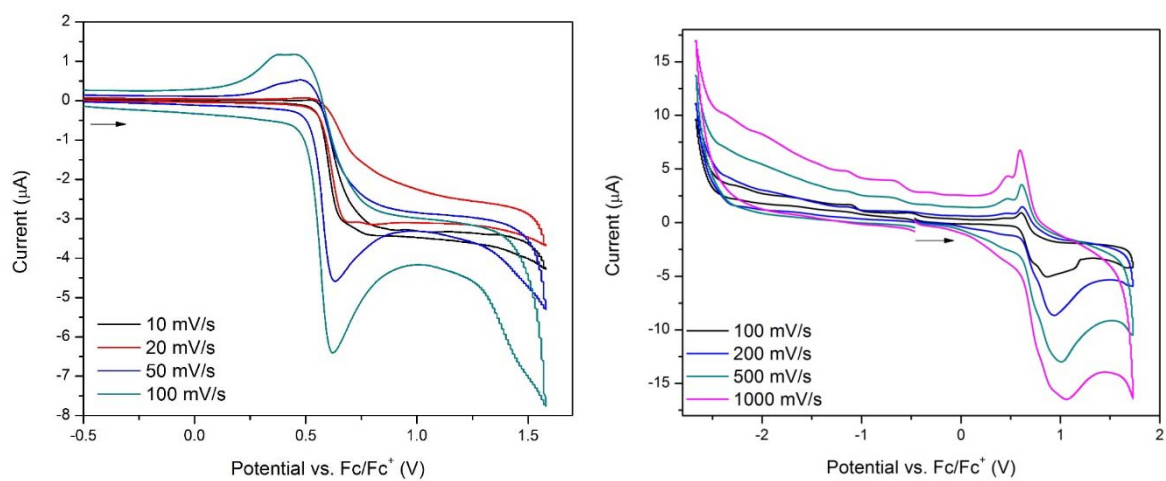


Figure S3. Solution state electrochemistry on **TPA-2bpm** in $[(n\text{-C}_4\text{H}_9)_4\text{N}]\text{PF}_6/\text{CH}_3\text{CN}$ electrolyte at scan rates of a) 10-100 mV/s and b) $[(n\text{-C}_4\text{H}_9)_4\text{N}]\text{PF}_6/\text{CH}_2\text{Cl}_2$ electrolyte at scan rates of 100-1000 mV/s where the arrow indicates the direction of the forward scan.

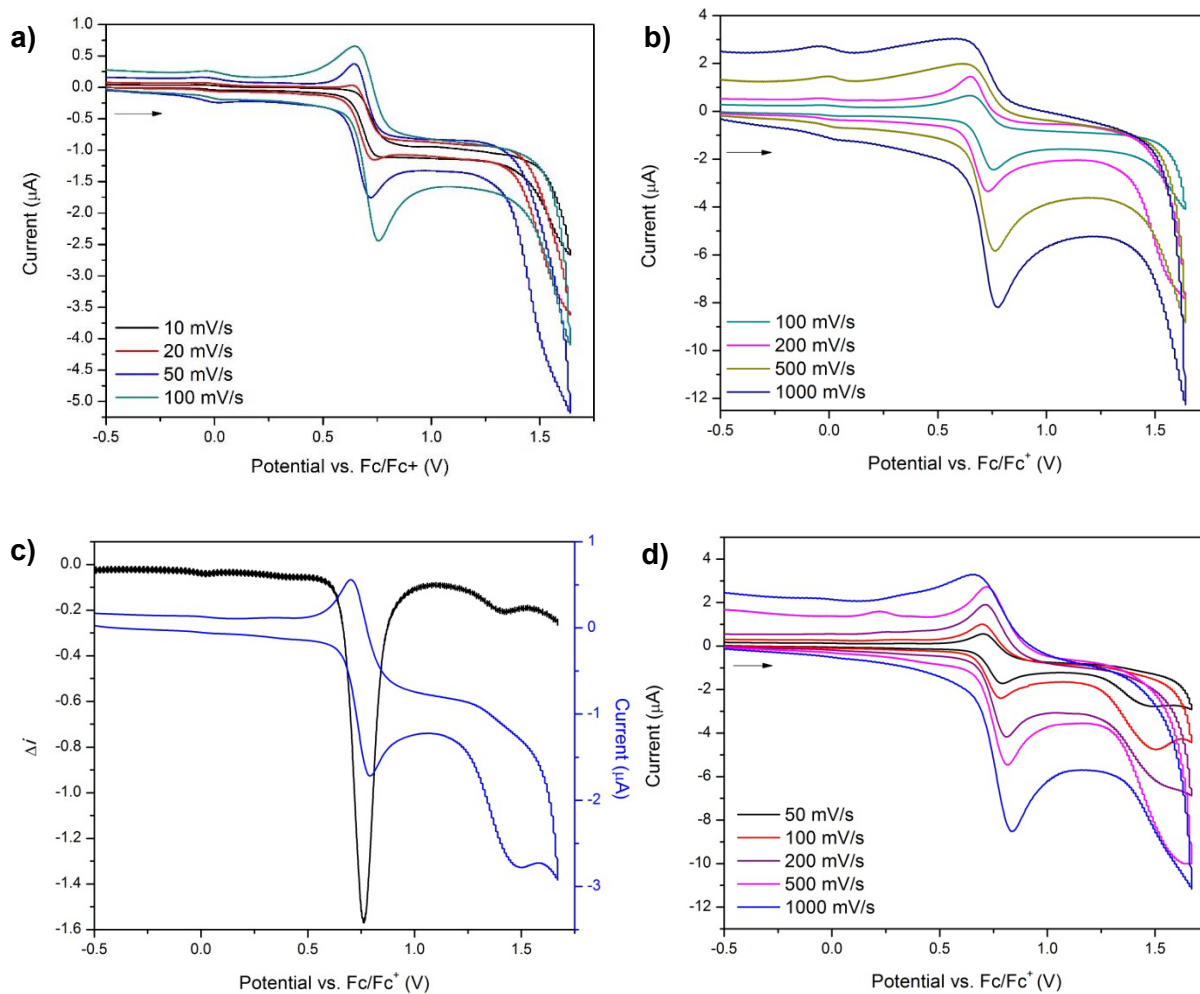


Figure S4. Solution state electrochemistry on **TPA-3bpm** in $[(n\text{-C}_4\text{H}_9)_4\text{N}]\text{PF}_6/\text{CH}_3\text{CN}$ electrolyte, referenced against the Fc/Fc^+ couple at scan rates of a) 10-100 mV/s, b) 100-1000 mV/s, c) square wave voltammogram at 10 mV and 39 Hz against the cyclic voltammogram at 50 mV/s and d) scan rates of 50-1000 mV/s in $[(n\text{-C}_4\text{H}_9)_4\text{N}]\text{PF}_6/\text{CH}_2\text{Cl}_2$ electrolyte.

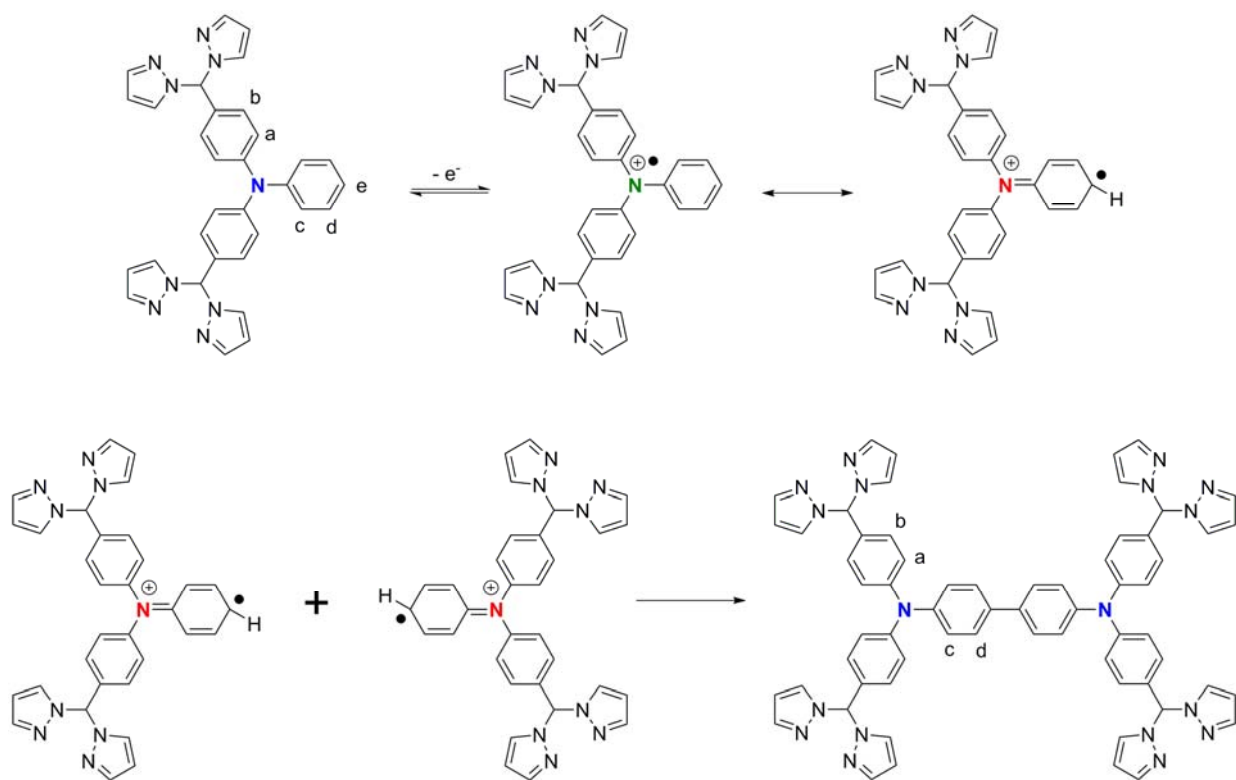


Figure S5. Mechanism of the dimerisation of TPA-2bpm upon oxidation to form the triarylamine radical cation.

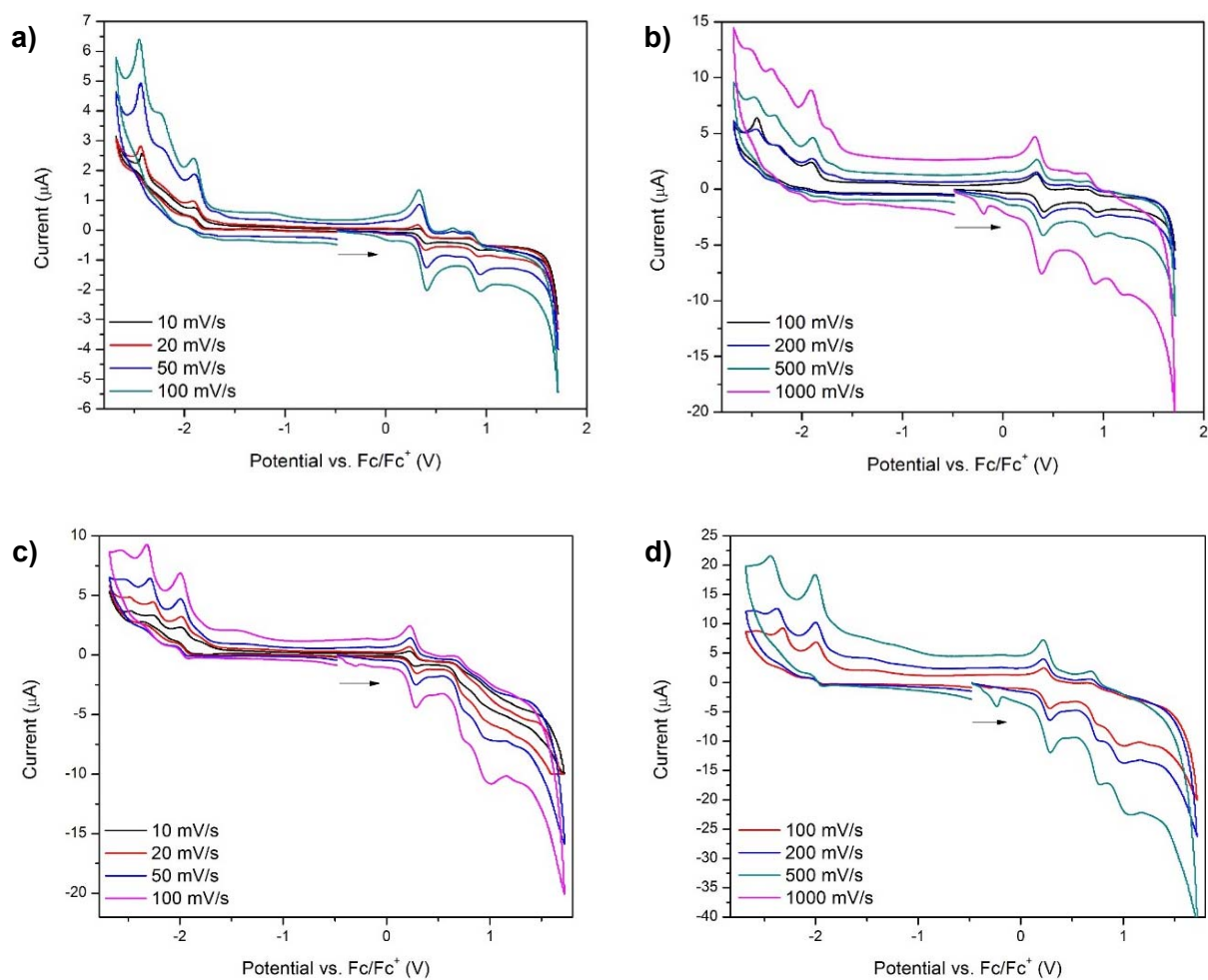


Figure S6. Cyclic voltammograms of $[\text{Ru}_2\text{Cl}_2(\text{tpy})_2(\text{TPA-2bpm})](\text{PF}_6)_2$ at scan rates of a) 10-100 mV/s and b) 100-1000 mV/s and $[\text{RuCl}(\text{tpy})(\text{TPA-3bpm})]\text{PF}_6$ at different scan rates where c) 10-100 mV/s and d) 100-1000 mV/s in $[(n\text{-C}_4\text{H}_9)_4\text{N}]\text{PF}_6/\text{CH}_3\text{CN}$ electrolyte.

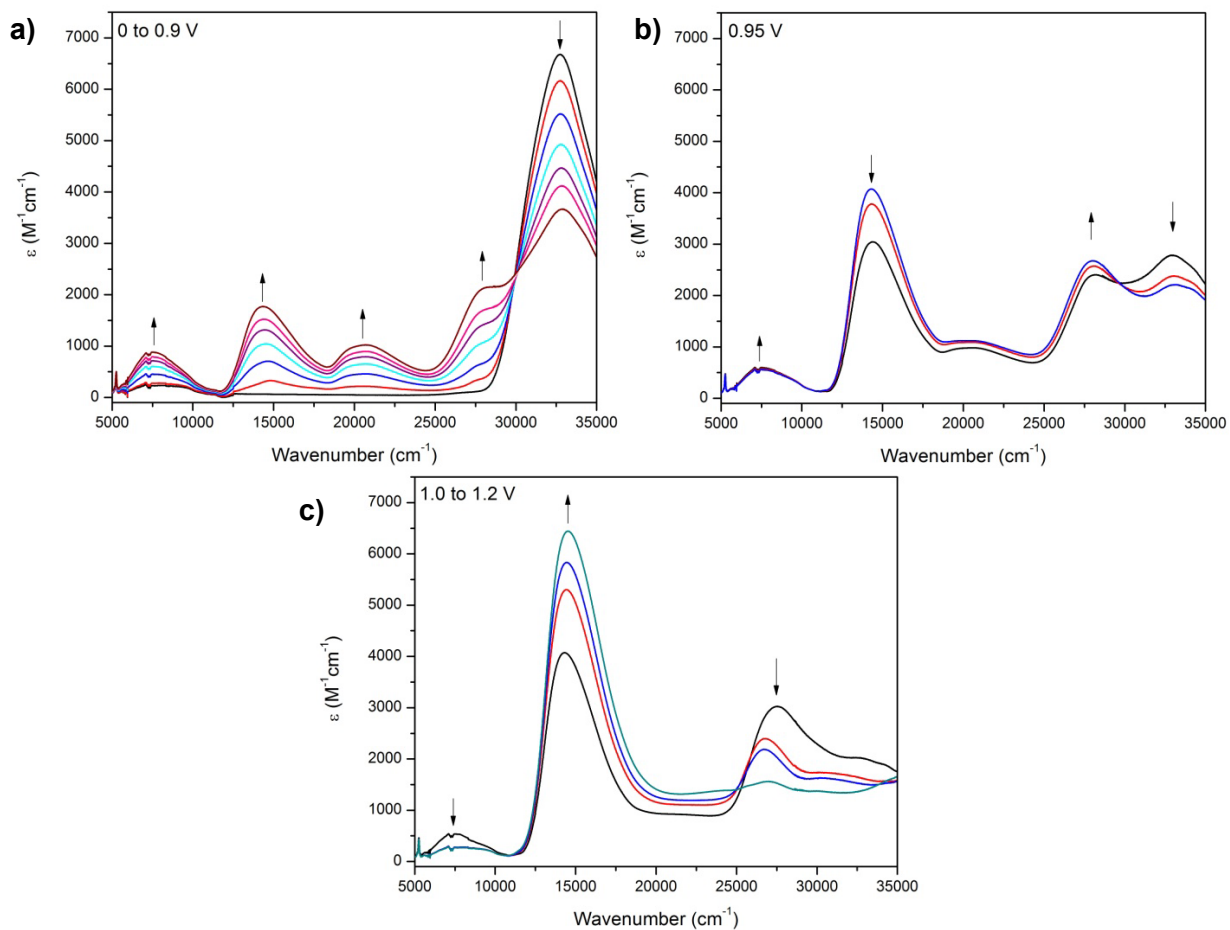


Figure S7. Solution state spectroelectrochemistry of TPA-2bpm in $[(n\text{-C}_4\text{H}_9)_4\text{N}]\text{PF}_6/\text{CH}_3\text{CN}$ electrolyte a) upon increasing the potential from 0 to 0.9 V, b) holding at 0.95 V and c) increasing the potential from 1.0 to 1.2 V.

Table S3. Parameters used in the IVCT analysis of the NIR bands of the TPA-2bpm ligand and $[\text{Ru}_2\text{Cl}_2(\text{tpy})_2(\text{TPA-2bpm})](\text{PF}_6)_2$.

	$\nu_{\text{max}}/\text{cm}^{-1}$	$\epsilon_{\text{max}}/\text{M}^{-1}\text{cm}^{-1}$	$\Delta\nu_{1/2}/\text{cm}^{-1}$	$\nu_{1/2}$ (high) $/\text{cm}^{-1}$	$\Delta\nu_{1/2}^\circ/\text{cm}^{-1}$	$H_{\text{ab}}/\text{cm}^{-1}$	$r_{\text{ab}}/\text{\AA}$
TPA-2bpm	7582	881	3325	1896	4185	337	9.72
$[\text{Ru}_2\text{Cl}_2(\text{tpy})_2(\text{TPA-2bpm})](\text{PF}_6)_2$	7783	2620	3495	1974	4240	566	9.72

Calculation of $\Delta\nu_{1/2}^\circ$ ¹⁻³

$$\begin{aligned}\Delta\nu_{1/2}^\circ &= [16RT \times \log_e(2) \times \nu_{\text{max}}]^{1/2} \\ &= [2310 \times \nu_{\text{max}}]^{1/2}\end{aligned}$$

Calculation of H_{ab} ¹⁻³

$$H_{\text{ab}} = 0.0206(\nu_{\text{max}} \times \epsilon_{\text{max}} \times \Delta\nu_{1/2})^{1/2} / r_{\text{ab}}$$

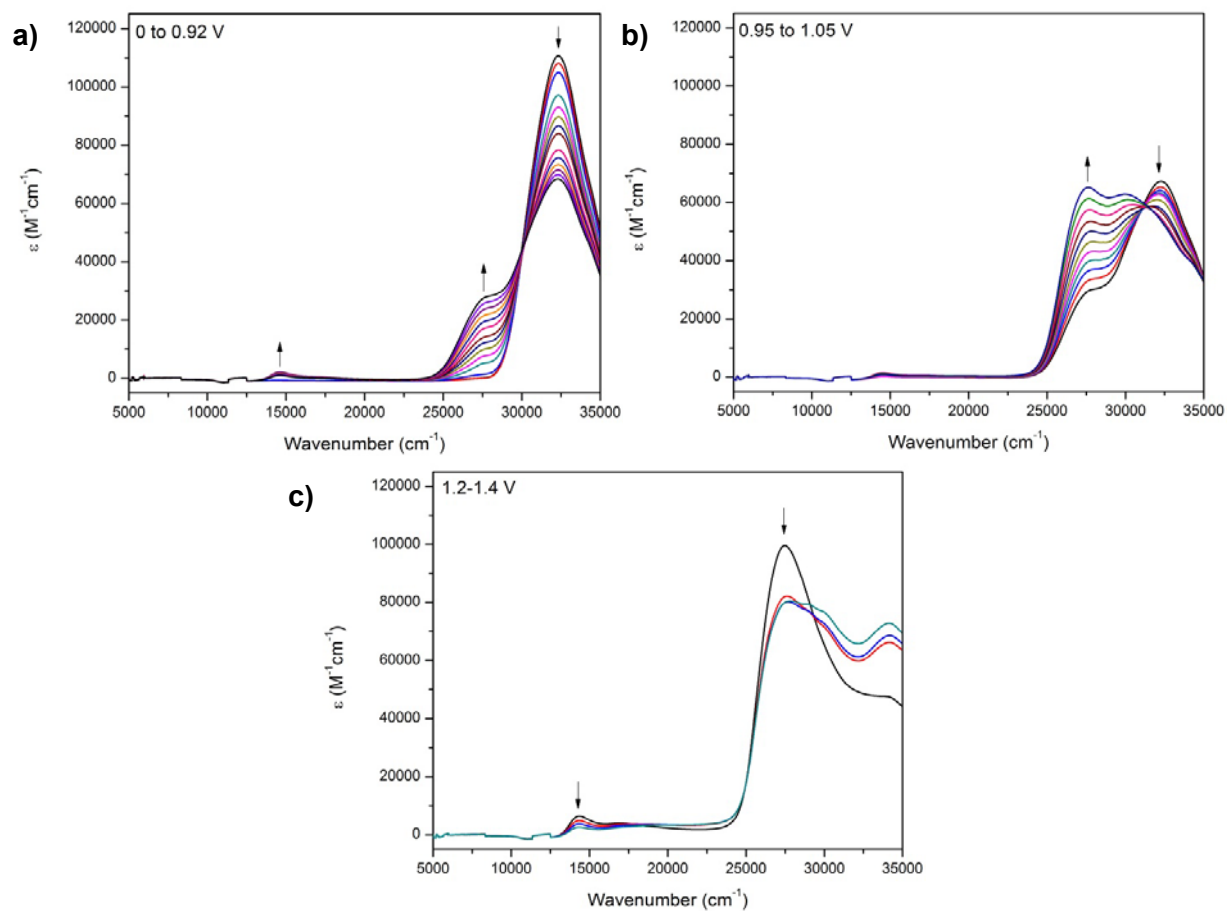


Figure S8. Solution state spectroelectrochemistry of TPA-3bpm in $[(n-C_4H_9)_4N]PF_6/CH_3CN$ electrolyte upon increasing the potential from a) 0 to 0.92 V, b) 0.95 to 1.05 V and c) 1.0 to 1.15 V.

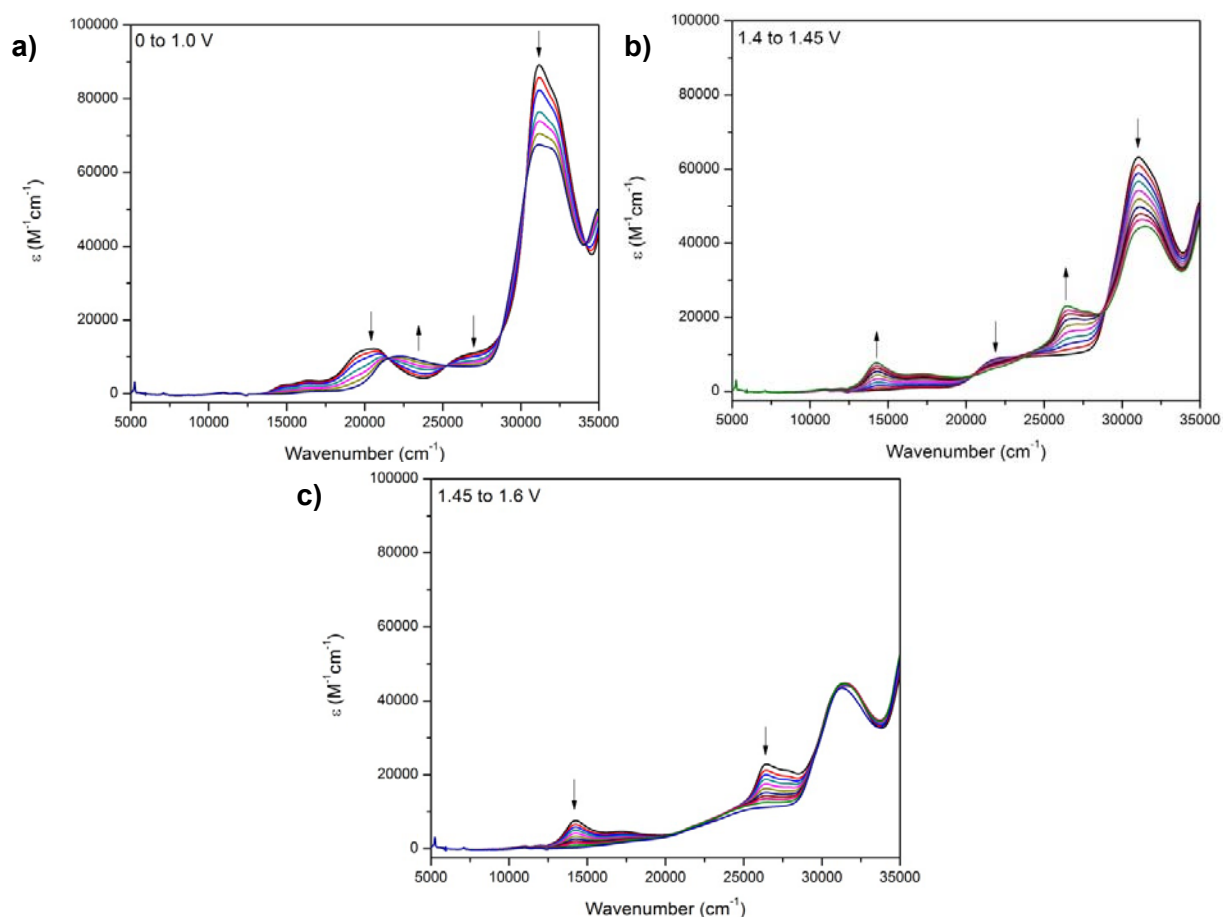


Figure S9. Solution state UV/Vis/NIR spectroelectrochemistry of $[\text{Ru}_3\text{Cl}_3(\text{tpy})_3(\text{TPA-3bpm})](\text{PF}_6)_3$ in $[(n\text{-C}_4\text{H}_9)_4\text{N}]\text{PF}_6/\text{CH}_3\text{CN}$ electrolyte where the potential was increased from a) 0 to 1.0 V, b) 1.4 to 1.45 V and c) 1.45 to 1.6 V.

Table S4. g -factor and hyperfine coupling values for the Ru(II) complexes containing the **TPA-3bpm** ligand.

Compound	g -factor	A (MHz) for N
$[\text{Ru}(\text{tpy})\text{Cl}(\text{TPA-3bpm})]\text{PF}_6$	2.0068	26.7
$[\text{Ru}_2(\text{tpy})_2\text{Cl}_2(\text{TPA-3bpm})](\text{PF}_6)_2$	2.0069	26.7
$[\text{Ru}_3(\text{tpy})_3\text{Cl}_3(\text{TPA-3bpm})](\text{PF}_6)_3$	2.0071	26.7

Table S5. Simulation parameters for the ^{14}N and ^1H nuclei in $[\text{Ru}(\text{tpy})\text{Cl}(\text{TPA-3bpm})]\text{PF}_6$ as a frozen solution at X-band and Q-band.

	g_x (N)	g_y (N)	g_z (N)	A (MHz)	Line Broadening (Voigtian)	g (H)	A (MHz)
X-band (5 K)	1.985	1.9985	2.0115	9.8	0.25, 0.25	1.9985	15.4
Q-band (50 K)	1.9915	1.9957	1.9995	9.8	0.25, 0.25	1.9957	15.4

Table S6. Simulation parameters for the ^{14}N and ^1H nuclei in $[\text{Ru}(\text{tpy})\text{Cl}(\text{TPA-3bpm})]\text{PF}_6$ as a solution at X-band.

Nucleus	g	A (MHz)	Correlation Time (s)	Line broadening (Voigtian)	No. Of Nuclei
N	2.0069	25.3	1×10^{-8}	0.45, 0.4	1
H	2.005	15.4		0, 0.1	6

Table S7. Simulation parameters for Ru^{3+} in $[\text{Ru}(\text{tpy})\text{Cl}(\text{TPA-3bpm})]\text{PF}_6$ as a frozen solution at X-band.

	$g_x(\text{Ru}^{3+})$	$g_y(\text{Ru}^{3+})$	$g_z(\text{Ru}^{3+})$	A_{\parallel} (MHz)	A_{\perp} (MHz)	Line Broadening (Voigtian)
X-band (5 K)	2.5	2.32	1.99	238	11.2	4.5, 4.5

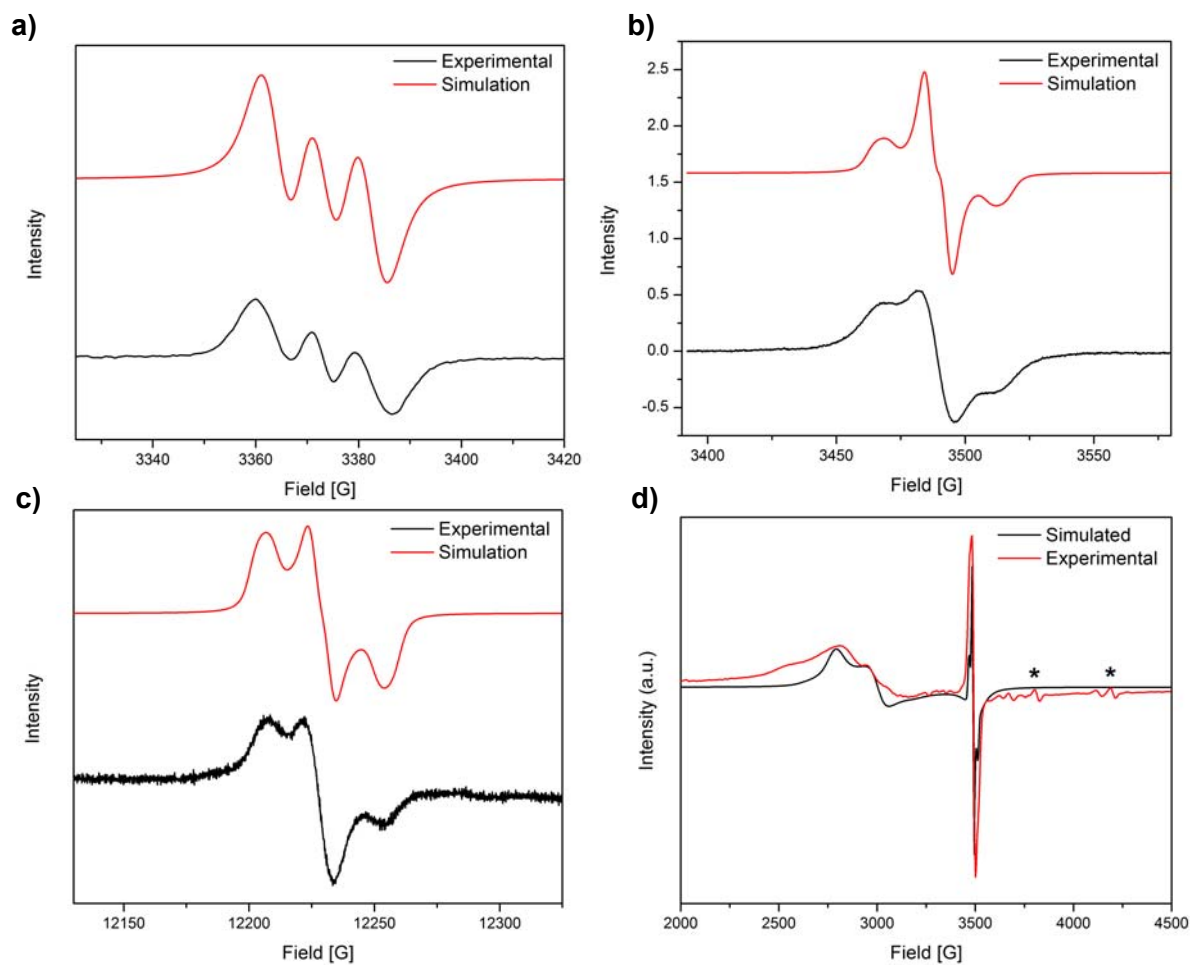


Figure S10. EPR spectroelectrochemistry of $[\text{Ru}(\text{tpy})\text{Cl}(\text{TPA-3bpm})]\text{PF}_6$ in $[(n\text{-C}_4\text{H}_9)_4\text{N}]\text{PF}_6/\text{CH}_3\text{CN}$ electrolyte showing the simulated vs. experimental spectrum of the radical a) in solution at 240 K at X-band, b) as a frozen solution at 5 K at X-band, c) as a frozen solution at 50 K at Q-band and d) the Ru^{3+} and radical at X-band at 5K where the signals indicated by * are due to the cavity.

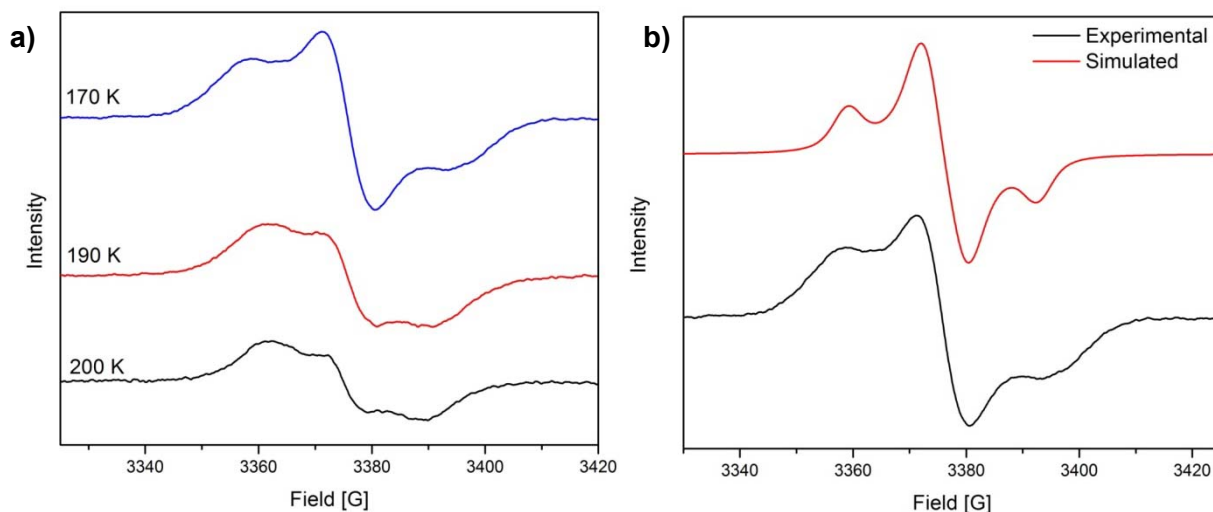


Figure S11. X-band EPR spectrum of the radical produced by the electrochemical experiment in $[(n\text{-C}_4\text{H}_9)_4\text{N}]\text{PF}_6/\text{CH}_2\text{Cl}_2$ electrolyte of **TPA-3bpm** a) at 170, 190 and 200 K and b) the simulated vs. experimental spectrum at 170 K as a frozen solution at a potential of 1.7 V.

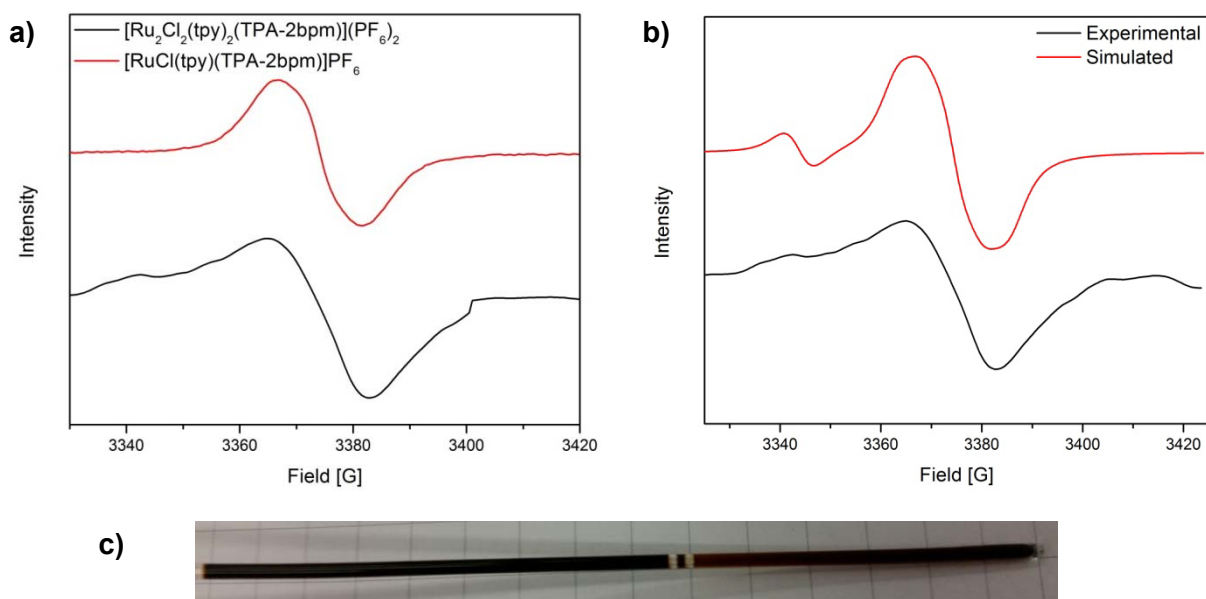


Figure S12. EPR spectroelectrochemistry in $[(n\text{-C}_4\text{H}_9)_4\text{N}]\text{PF}_6/\text{CH}_3\text{CN}$ electrolyte of a) $[\text{Ru}(\text{tpy})\text{Cl}(\text{TPA-2bpm})](\text{PF}_6)$ and $[\text{Ru}_2(\text{tpy})_2\text{Cl}_2(\text{TPA-2bpm})](\text{PF}_6)_2$, b) simulated vs. experimental spectrum of $[\text{Ru}_2(\text{tpy})_2\text{Cl}_2(\text{TPA-2bpm})](\text{PF}_6)_2$ and c) photo of $[\text{Ru}_2(\text{tpy})_2\text{Cl}_2(\text{TPA-2bpm})](\text{PF}_6)_2$ during the experiment.

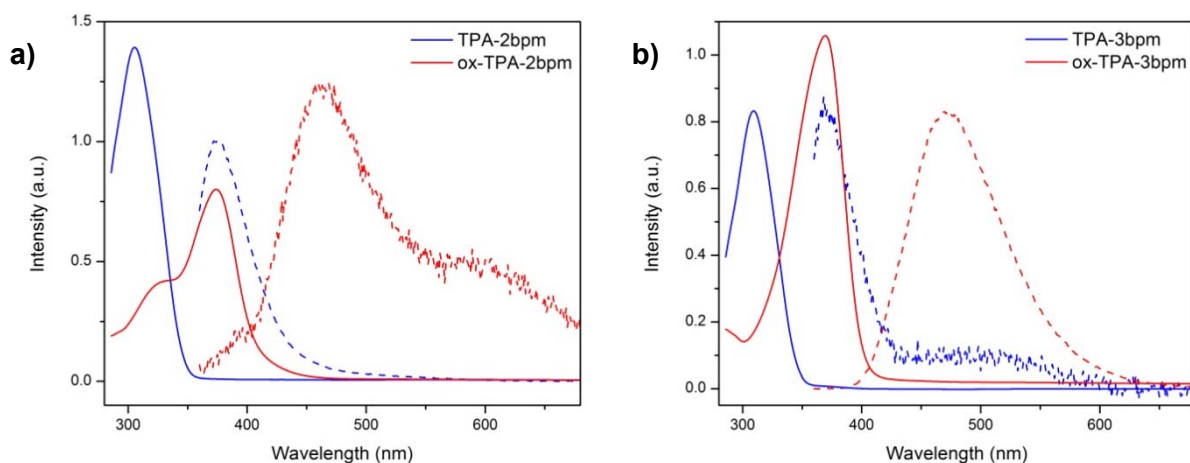


Figure S13. Absorbance and fluorescence spectra of a) TPA-2bpm, ox-TPA-2bpm and b) TPA-3bpm, ox-TPA-3bpm as solutions in acetonitrile.

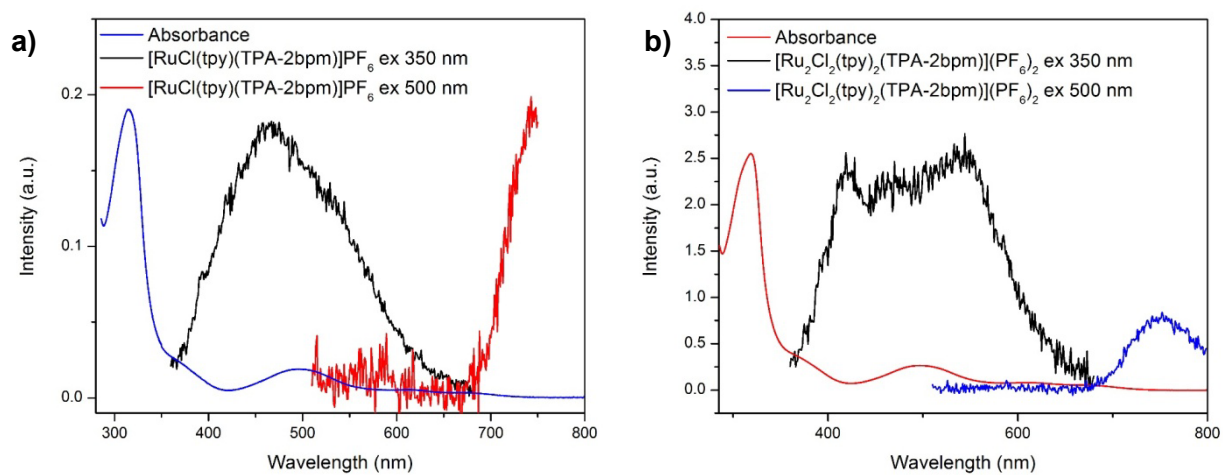


Figure S14. Absorbance and fluorescence spectra of a) $[\text{RuCl}(\text{tpy})(\text{TPA-2bpm})]\text{PF}_6$ and b) $[\text{Ru}_2\text{Cl}_2(\text{tpy})_2(\text{TPA-2bpm})](\text{PF}_6)_2$ upon excitation at 350 (28570 cm^{-1}) and 500 nm (20000 cm^{-1}).

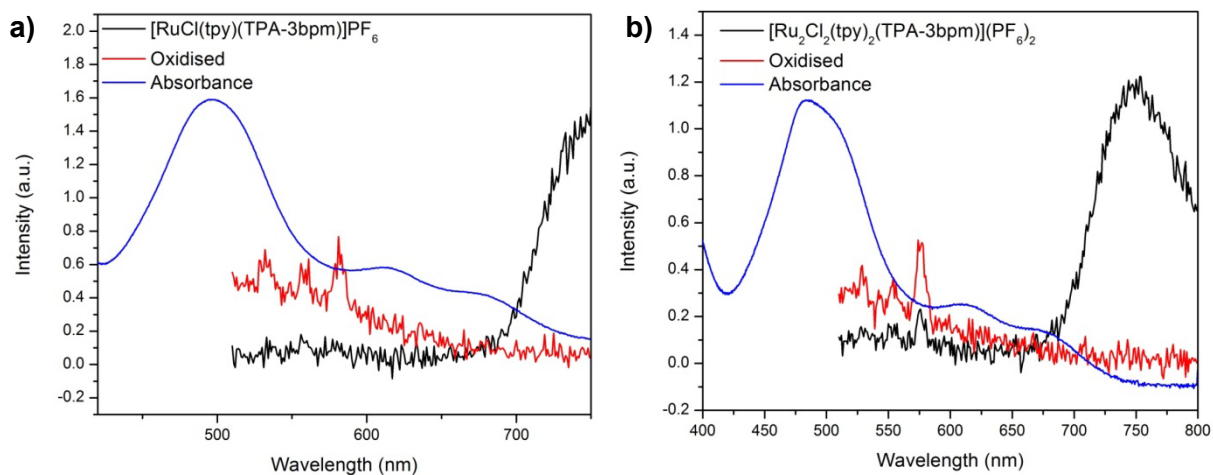


Figure S15. Absorbance and fluorescence spectra of a) $[\text{RuCl}(\text{tpy})(\text{TPA-3bpm})]\text{PF}_6$ and b) $[\text{Ru}_2\text{Cl}_2(\text{tpy})_2(\text{TPA-3bpm})](\text{PF}_6)_2$ and their oxidised species upon excitation at 490 nm (no fluorescence at 320 nm).

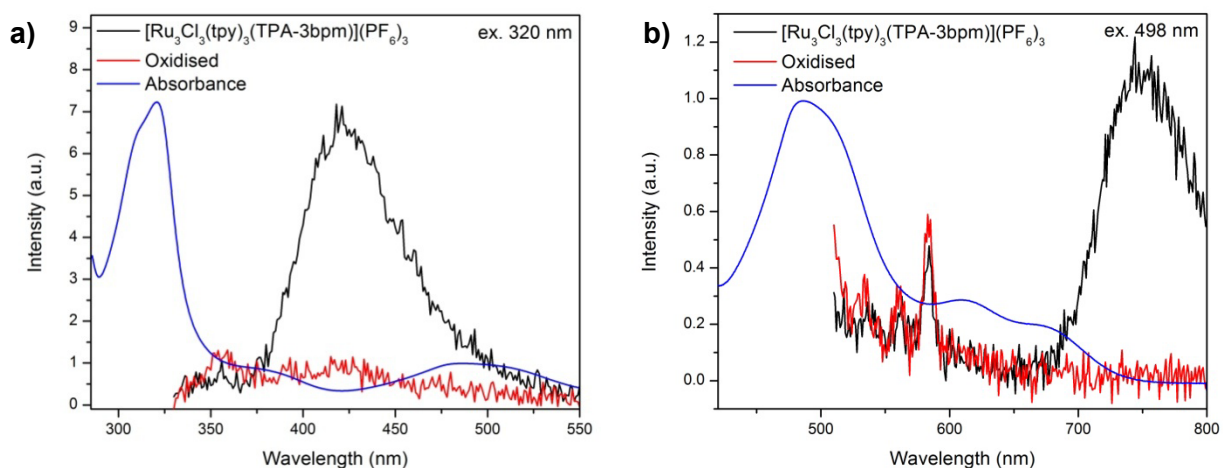


Figure S16. Absorbance and Fluorescence spectra of $[\text{Ru}_3\text{Cl}_3(\text{tpy})_3(\text{TPA-3bpm})](\text{PF}_6)_3$ upon excitation at 320 nm and 495 nm.

References

1. Hush, N. S., Intervalence-Transfer Absorption. Part 2. Theoretical Considerations and Spectroscopic Data. In *Prog. Inorg. Chem.*, John Wiley & Sons, Inc.: 2007; pp 391-444.
2. Hush, N. S., *Electrochim. Acta* **1968**, *13*, 1005-1023.
3. D'Alessandro, D. M.; Keene, F. R., *Chem. Soc. Rev.* **2006**, *35*, 424-440.